RelB-deficient autoinflammatory pathology presents as interferonopathy, but in mice is interferon-independent

Héctor I. Navarro, PhD,[a,b] Yi Liu, PhD,[a,b,c] Anna Fraser, BS,[a,b,d] Diane Lefaudeux, MEng,[a,d] Jennifer J. Chia, MD, PhD,[a,b,e] Linda Vong, PhD,[f] Chaim M. Roifman, CM, MD, FRCPC, FCACB,[f] and Alexander Hoffmann, PhD[a,b,d]   *Los Angeles, Calif; Beijing, China; and Toronto, Ontario, Canada*

Background: Autoimmune diseases are leading causes of ill health and morbidity and have diverse etiology. Two signaling pathways are key drivers of autoimmune pathology, interferon and nuclear factor-κB (NF-κB)/RelA, defining the 2 broad labels of interferonopathies and relopathies. Prior work has established that genetic loss of function of the NF-κB subunit RelB leads to autoimmune and inflammatory pathology in mice and humans.

Objective: We sought to characterize RelB-deficient autoimmunity by unbiased profiling of the responses of immune sentinel cells to stimulus and to determine the functional role of dysregulated gene programs in the RelB-deficient pathology.

Methods: Transcriptomic profiling was performed on fibroblasts and dendritic cells derived from patients with RelB deficiency and knockout mice, and transcriptomic responses and pathology were assessed in mice deficient in both RelB and the type I interferon receptor.

Results: We found that loss of RelB in patient-derived fibroblasts and mouse myeloid cells results in elevated induction of hundreds of interferon-stimulated genes. Removing hyperexpression of the interferon-stimulated gene program did not ameliorate the autoimmune pathology of RelB knockout mice. Instead, we found that RelB suppresses a different set of inflammatory response genes in a manner that is independent of interferon signaling but associated with NF-κB binding motifs.

Conclusion: Although transcriptomic profiling would describe RelB-deficient autoimmune disease as an interferonopathy, the genetic evidence indicates that the pathology in mice is interferon-independent. (J Allergy Clin Immunol 2023;152:1261-72.)

Autoimmune diseases and autoinflammatory diseases are rapidly expanding categories of immune-related disorders and a major health concern. Current studies estimate that there are around 150 lifelong debilitating autoimmune diseases characterized by a dysregulation of adaptive immune system and no known cures,[1] as well as a growing list of 40 genetically described auto-inflammatory diseases characterized by a dysregulation of the innate immune system.[2] These diseases have chronic lifelong symptoms such as chronic fevers,[3] arthritis,[4] inflammatory bowel disease,[5] and hepatic and central nervous system inflammation,[6,7] among other serious health issues. Our understanding of the role of chronic inflammation in other human diseases such as cancer, heart disease, and psychiatric disorders is also growing rapidly.[8] Therefore, understanding autoimmune and autoinflammatory diseases is critically important to therapeutically addressing the growing number of patients with autoimmune and autoinflammatory diseases, as well as other human diseases in which inflammation plays a key role. Autoinflammatory diseases have recently been categorized into the following 5 subsets based on underlying dysregulated mechanisms: inflammasomopathies, interferonopathies, unfolded protein responses/endoplasmic reticulum stress syndromes, relopathies, and uncategorized.[9]

Of growing interest are interferonopathies, which are defined as diseases grouped by mendelian disorders associated with an upregulation of type I interferon that were first described in 2003[10] and later officially categorized and termed.[11] Type I interferons are a class of antiviral, anti-inflammatory proteins first discovered in 1957 for their ability to induce influenza viral interference.[12] Type I interferons signal in a paracrine and autocrine manner via the IFN-α/β receptor (IFNAR), which comprises 2 subunits, IFNAR1 and IFNAR2. The interferon receptor has been shown to be expressed by virtually every nucleated cell of both hematopoietic and nonhematopoietic origin, and although some cells are specialized producers of type I interferon, almost all cells are able to produce type I interferon.[13] After type I interferon binding to the IFNAR receptor, a downstream transcription factor complex, ISGF3, is formed and induces the expression of interferon-stimulated genes (ISGs) by binding to their promoter regions containing interferon-sensitive response elements (ISREs). Given the broad extent of the interferon signaling network in human physiology, as one might expect, dysregulation of interferon signaling leads to a multitude of pathologies affecting various organs and organ systems. For example, *USP18$^{-/-}$* mice, which lack a negative regulator of interferon signaling (ie, UBP43, which leads to elevated levels of conjugates

Abbreviations used

DC:	Dendritic cell
FC:	Fold change
GO:	Gene Ontology
IFNAR:	IFN-α/β receptor
ISG:	Interferon-stimulated gene
ISRE:	Interferon-sensitive response element
MC:	Myeloid cell
M-CSF:	Macrophage colony-stimulating factor
MCSF MC:	Myeloid cell differentiated with macrophage colony-stimulating factor
RNA-seq:	RNA sequencing
TLR:	Toll-like receptor
TSS:	Transcription start site
UCLA:	University of California, Los Angeles
WT:	Wild-type

to ISG15, a potently induced ISGF3 target gene), develop brain injury accompanied by hydrocephalus and early death, with 50% such of mice dying at age 4 weeks.[14,15] This pathology was also seen in human patients with ISG15 null mutations, causing death or seizures in 3 patients.[16] Interferonopathies can cause other harmful effects on the central nervous system, such as epilepsy, as well as psychomotor retardation in Aicardi-Goutières syndrome,[17] and they have also been shown to lead to interstitial lung disease, arthritis, panniculitis lipodystrophy, necrotizing vasculitis, bone dysplasia, and early thrombotic events, among other serious symptoms.[18] Importantly, although we can broadly categorize autoinflammatory diseases into interferonopathies, the pathologic outcomes and symptoms of diseases within this category vary broadly and often have overlapping dysregulation of various immune-related signaling pathways. Many autoinflammatory diseases also share autoimmune disease characteristics involving dysregulation in both innate and adaptive immunity. Therefore, understanding the underlying mechanisms and etiology of these pathologies in a disease-specific manner is crucial to effectively tailoring therapeutic approaches for patients with highly unique genetic lesions.

Recently, pediatric patients with a homozygous null mutation in the gene encoding the NF-κB subunit RelB were described.[19-21] These patients presented a combined immunodeficiency phenotype with failure to thrive and a significantly impaired ability to produce specific antibodies *in vivo.*[20] Interestingly, these patients were also characterized by an autoimmune pathology presenting as severe autoimmune skin disease and rheumatoid arthritis involving altered thymic T-cell maturation with reduced output and production of a skewed T-cell repertoire with expansion of clones.[21] Although defects in the adaptive immune system were found and well described in these studies, the description of the patient innate immune function was more limited but appeared to behave normally relative to adaptive immune system, as measured by TNF secretion in patient-derived monocytes. However, patient-derived fibroblasts, which are key pathogen-sensing sentinel cells, were revealed to have elevated TNF-induced RelA DNA-binding activity.[21]

Findings in the RelB-null human pathology bore a striking resemblance to previously reported phenotypes of *RelB*^{−/−} mice (multiorgan inflammation, thymic atrophy, reduction of thymocytes, and impaired cell-mediated immune response but normal T- and B-cell development),[22] suggesting consistent mechanisms between human and mouse pathology. In mice, functional adoptive transfer studies identified dendritic cells (DCs), which are key pathogen-sensing immune sentinel cells, to be key drivers of the lung inflammatory pathology seen in *RelB*^{−/−} mice.[23] Another study supported these findings by demonstrating restoration of the thymic atrophy and the numbers of thymic Foxp3^{+} regulatory T cells in *RelB*^{−/−} mice after adoptive transfer of *RelB*[+] DCs.[24] However, subsequent studies addressing the autoinflammatory mechanisms that cause immune sentinel cells to drive the pathology have reported several different mechanisms, and no consensus has emerged.[25-27]

We aimed to further understand the mechanistic dysregulation of RelB-null immune sentinel cells as they contribute to *RelB*^{−/−} autoinflammatory disease. Given recent reports of elevated interferon signaling caused by RelB deficiency,[28-30] we hypothesized that dysregulation of the interferon pathway may be present in RelB-null patient-derived sentinel cells, potentially implying immediate clinically relevant characterization of the RelB null pathology as an interferonopathy. Indeed, we found that loss of RelB in patient-derived fibroblasts and mouse DCs, but not macrophages, results in elevated expression of ISGs that is dependent on elevated type I interferon signaling. To our surprise, however, although the hyperexpression of ISGs is a prominent aspect of the loss of RelB phenotype, complete ablation of type I interferon signaling in the mouse did not ameliorate the RelB pathology. We found instead that RelB directly suppresses a myriad of interferon-independent proinflammatory and immune response genes promoting a cell-intrinsic hyperactivated inflammatory state both in *RelB*^{−/−} human fibroblasts and mouse DCs, which in turn are likely key contributors to the RelB-null autoimmune and autoinflammatory pathology.

METHODS
Patient-derived fibroblasts

Total RNA was prepared as described.[31] Strand-specific libraries were generated from 200 ng of total RNA by using the KAPA Stranded mRNA sequencing and Library Preparation Kit (Illumina, San Diego, Calif). cDNA libraries were single-end sequenced (50 bp) on an Illumina HiSeq 2000. RNA sequencing (RNA-seq) reads were trimmed by using cutadapt, version 1.12,[31] to remove low-quality ends and the remaining adapter sequence. The reads were then aligned on the human genome (hg38) by using STAR software v2.5.2b.[32] The aligned reads were filtered by using samtools version 1.3.1[33] to keep only uniquely aligned reads. Gene expression quantification was done by using featureCounts, version 1.5.1,[34] and GENCODE, version 23, gene annotation.[35] Differentially expressed genes were selected by using edgeR[36] with a 4-fold and 0.01 false discovery rate threshold in either wild-type (WT) or patient samples.

Clustering of differentially expressed genes was done by using a k-mean method to identify clusters of differentially expressed genes with similar dynamic profiles. Gene ontology (GO) and motif analysis were done via HOMER suite by considering regulatory regions within −4 kb to +1 kb from the transcription start site (TSS).
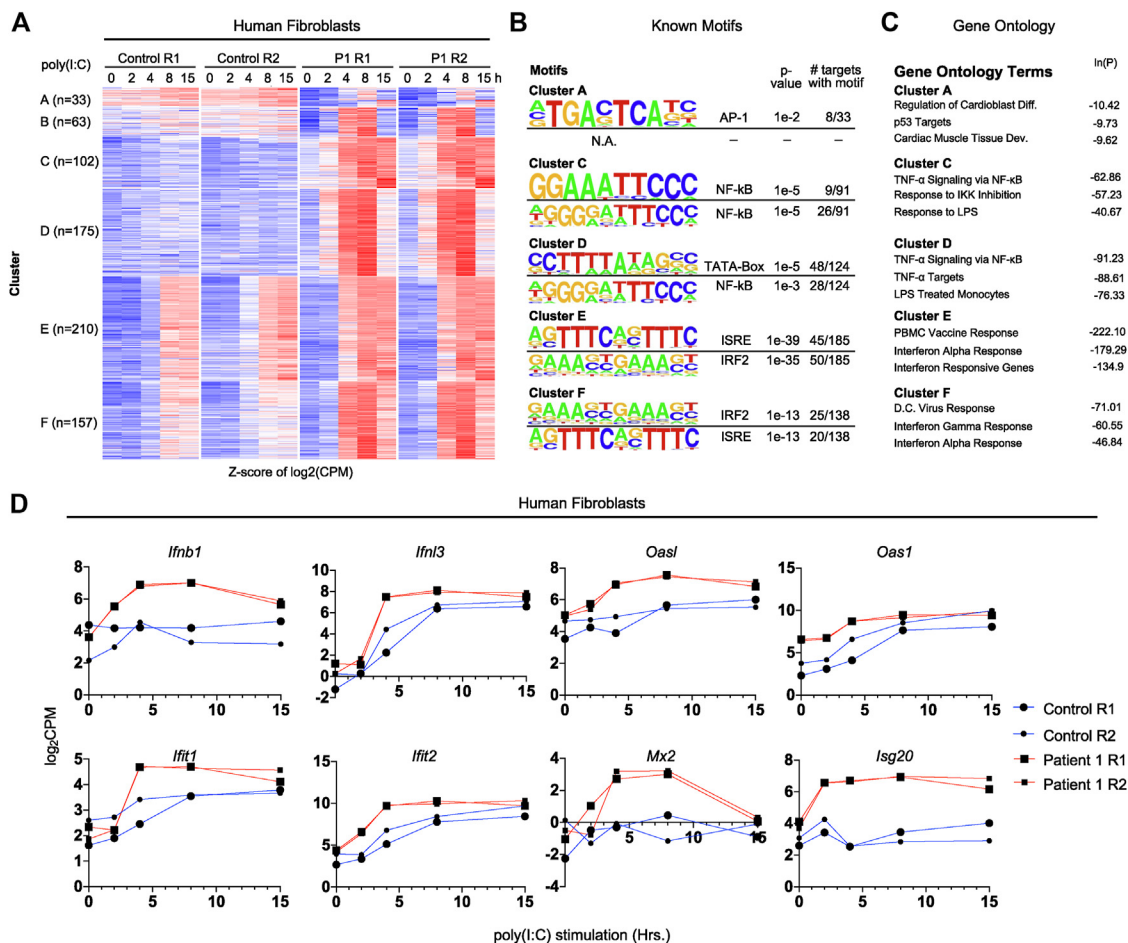
FIG 1. Fibroblasts obtained from a human RelB-null donor show hyperexpression of type I interferon and interferon-stimulated genes. **A,** Heatmap of *z*-scored log$_2$ cpm values of all poly(I:C)-induced (10 μg/mL; FC > 4; false discovery rate < 0.01) genes in control fibroblasts or fibroblasts derived from patient 1 (RelB-null) (740 genes). Each row represents individual genes, and each column is from an individual time point after stimulation. R1 and R2 are experimental replicates. Red and blue represent distance from the mean log$_2$ cpm value for each gene. **B,** Top 2 results of known motif analysis results for gene clusters from (**A**). Motif analysis considered regions within –4 kb to +1 kb from the TSS. Cluster B did not generate motifs with given parameters. **C,** GO results for gene clusters from (**A**). **D,** Line graphs of gene expression (log$_2$ cpm value) for *Ifn-β*, *Ifn-λ3*, and several ISGs during poly(I:C) stimulation (at 0, 2, 4, 8, and 15 hours). Large circle represents R1, small circle represents R2, red line represents fibroblasts derived from patient 1, large square represents R1, and small square represents R2. *N.A.*, No motif result.

Mice and bone marrow–derived DCs

WT and transgenic mice were housed in pathogen-free conditions at the University of California, Los Angeles (UCLA, Los Angeles, Calif). *RelB*$^{-/-}$ mice were generated by breeding *RelB*$^{+/-}$ mice, and *IFNAR*$^{-/-}$*RelB*$^{-/-}$ mice were generated by mating *IFNAR*$^{-/-}$*RelB*$^{+/-}$ or *IFNAR*$^{+/-}$*RelB*$^{+/-}$ mice with each other. All of the mice used for RNA-seq experiments were between 6 and 12 weeks of age on the day of the experiment. Both male and female mice were used for experiments. Bone marrow cells were isolated from mouse femurs and cultured with macrophage colony-stimulating factor (M-CSF)-containing L929-conditioned medium for bone marrow–derived macrophages or with 20 ng/mL of GM-CSF and 10 ng/mL of IL-4 to produce bone marrow–derived dendritic cells, with half the media being replaced on days 3 and 6 as previously reported.[37] Cells were stimulated with CpG (0.1 μM) (ODN 1668; catalog no. tlrl-1668, Invivogen, San Diego, Calif) or

Poly(I:C) HMW (10 μg/mL) (Invivogen; catalog no. tlrl-pic) and collected at specified time points in Invitrogen TRIzol reagent (catalog no. 15-596-018, Thermo Fisher Scientific Waltham, Mass). RNA was extracted by using the Qiagen RNeasy Mini Kit (catalog no. 74106, Qiagen Hilden, Germany) as described.[38]

Transcriptome profiling

RNA was used for Illumina bead arrays as described[31] and for RNA-seq as described.[39] Briefly, libraries were prepped by using the KAPA Stranded mRNA-Seq Kit Illumina platform KR0960, version 3.15, by using 1 μg of RNA per sample measured with a Qubit 2.0 fluorometer (Thermo Fisher Scientific). Final libraries were checked via agarose gel and multiplexed with a maximum of 24 samples per sequencing reaction. Libraries were sequenced using a Illumina HiSeq

FIG 2. Loss of RelB in mouse myeloid cells recapitulates hyperexpression of type I interferon and interferon-stimulated gene programs. **A,** Heatmap of *z*-scored mRNA expression of all Pam3CSK4-induced (500 ng/mL; log FC > 1) genes in WT GM-CSF MCs (425 genes) *(upper panel)*. Motif analysis and GO results for gene clusters from (**A**). *(lower panel)*. **B,** Line graphs of mRNA expression during Pam3CSK4 stimulation (at 0, 1, 3, 8, and 24 hours), blue line *(circle)* represents WT GM-CSF MCs, and red line *(square)* represents *RelB$^{-/-}$* GM-CSF MCs. **C,** *(top)* Heatmap of *z*-scored mRNA expression of all CPG-induced (0.1 μM; log FC > 1) genes in WT MCs (415 genes). *(bottom)* Motif analysis and GO results for gene clusters from (**C**). **D,** Line graphs

3000 with single-end 50-bp reads at the UCLA Technology Center for Genomics & Bioinformatics.

Bioinformatic analysis

Reads were trimmed using cutadapt[31] (cutoff $q = 20$) and mapped to the mm10 genome. Processed reads showed high-quality reads and alignment scores. The October 2014 version of the Ensembl database was used to extract gene annotation information. Count per minute (cpm) values were generated using edgeR[36] to normalize the raw counts data based on sequencing depth. To permit fold change (FC) calculations, a pseudocount of 1 cpm was added. Induced genes were selected by using a cutoff of log$_2$ FC greater than 1 for any stimulated time point relative to the hour 0 unstimulated control; transcripts with empty gene names were removed. Data were z-scored and plotted using the pheatmap R package. Fold differences of genes within heatmaps were calculated by first calculating the fold differences for all individual genes between the genotype of interest and the WT or *IFNAR*^{−/−} control cpm value (genotype X) divided by the cpm value (genotype Y) for each individual time point. Average fold differences were then calculated by averaging the fold differences of all genes within each cluster for each individual time point. GO and motif analysis was done via homer suite with consideration for regulatory regions within −1 kb to +1 kb from the TSS. Line graphs of individual genes were generated using Graph-Pad Prism.

Tissue isolation and fixation

Spleens were isolated from age-matched mice immediately after they had been humanely killed and subsequently rinsed with PBS. Excess PBS was removed from the mouse spleens, which were subsequently weighed. Fixation was done in 10% formaldehyde for 46 to 48 hours. Tissue was processed, sectioned, and hematoxylin and eosin–stained by the UCLA Translational Pathology Core Laboratory.

Research ethics board approval

All patient studies were approved by the The Hospital for Sick Children Research Ethics Board (Protocol no. 1000005598).

RESULTS

Fibroblasts obtained from a human RelB-null donor show hyperexpression of type I interferon and interferon-stimulated genes

To characterize the transcriptome-wide defects caused by the loss of RelB, we performed an unbiased differential gene expression analysis by using fibroblasts obtained from a previously reported patient with combined immunodeficiency (patient 1) with an autoimmune disease pathology arising as a consequence of a rare homozygous mutation in the *RelB* gene resulting in complete

loss of the RelB protein and fibroblasts from a healthy close relative of that patient with homozygous copies of WT *RelB* (control).[20,21] To experimentally model immune stimulation via pattern recognition receptors that may occur in response to pathogen exposure or tissue injury, we stimulated fibroblasts with the Toll-like receptor 3 (TLR3) agonist poly(I:C) (10 μg/mL) in replicate. After collecting RNA at 5 time points (0, 2, 4, 8, and 15 hours), we performed whole transcriptome RNA-seq and bioinformatically identified 740 genes that were induced with a FC greater than 4 and false discovery rate less than the 0.01 threshold in either WT replicate samples or replicate samples from patient 1. Applying k-means clustering to the expression data of these genes, we identified 6 distinct clusters of differentially expressed genes that were hyperexpressed in patient1 (Fig 1, *A*). A small proportion of the genes clustered within cluster A (33 genes) and cluster B (63 genes) but resulted in weak or no motif enrichment results; however, most genes of the clustered in hyperexpressed clusters C through F, which were revealed to have average fold differences in cpm values ranging from 1.6× and 14× between the fibroblasts from patient 1 and the control fibroblasts at any of the measured time points (Fig 1, *A* and see Table E1 in the Online Repository at www.jacionline.org). To identify potential regulatory features of these genes, we performed a motif enrichment analysis that considered regions within −4 kb to +1 kb from the TSS of the regulatory region of each gene. Genes within the hyperexpressed clusters C (102 genes) and D (175 genes) were statistically enriched for NF-κB motifs in regulatory regions, whereas hyperexpressed clusters E (210 genes) and F (157 genes) were statistically enriched for IRF and ISRE motifs (Fig 1, *B*). This analysis suggested 2 major categories of dysregulated genes: ISGs and NF-κB–regulated genes. To identify potential biologic functions, we performed gene ontology (GO) analysis. Clusters C and D were associated with terms invoking NF-κB–activating pathways such as *TNF* and *LPS signaling*. Clusters E and F were associated with terms invoking interferon-inducing pathways, including *type I IFN-α response* and *type II IFN-γ response* (Fig 1, *C*). Analysis of individual genes within clusters E and F revealed many hyperexpressed ISGs, including *Oasl, Oas2, Ifit1, Ifit2, Mx2,* and *Isg20* (Fig 1, *D*). Given that ISGs may be activated by types I, II, and III interferons,[40] we evaluated the expression of interferon family members. We found *Ifnb1* and *Ifnl3* to be hyperexpressed in fibroblasts derived from patient 1 (Fig 1, *D*). Together, these data establish that loss of function of RelB results in hyperinduction of not only NF-κB–associated genes but also a large ISG expression program, prompting the question of whether it drives the described autoimmune/autoinflammatory pathology.

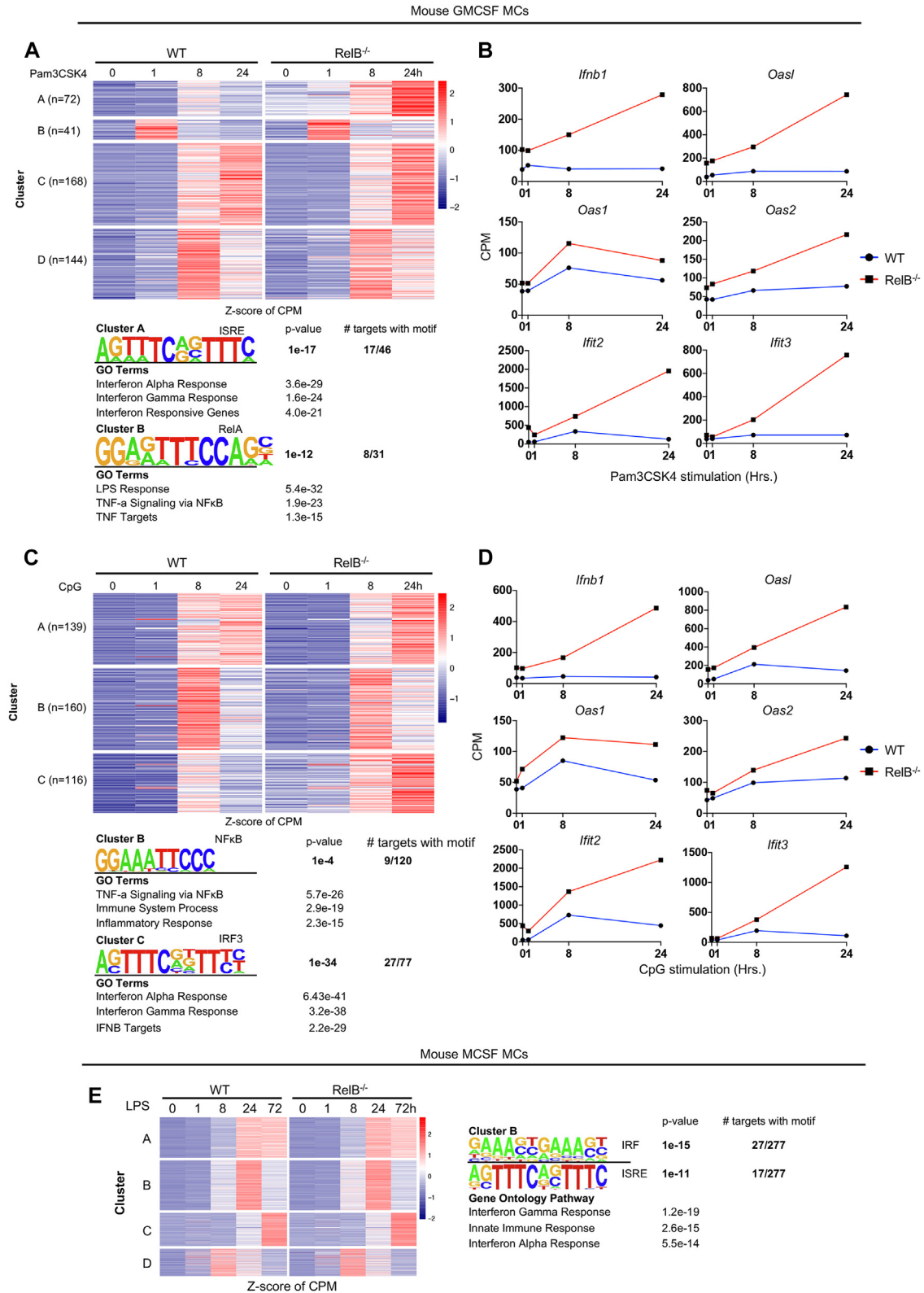### Loss of RelB in mouse myeloid cells recapitulate the hyperexpression of type I interferon and interferon-stimulated gene programs observed in patient fibroblasts

Adoptive transfer studies suggested that myeloid cells (MCs) play a key role in driving the lethal multiorgan inflammation in *RelB*^{−/−} mice.[23,24] We therefore undertook transcriptomic

---

of mRNA expression during CpG stimulation (at 0, 1, 3, 8, and 24 hours). Same color key as in (**B**). **E,** (*left*) Heatmap of z-scored mRNA expression of all LPS-induced (log FC > 1) genes in WT or *RelB*^{−/−} MCSF MCs (1,243 unique genes). **E,** (*right*) Motif analysis and GO results from gene cluster B. Each row in the heatmaps represents individual genes, and each column is an individual time point during stimulation. Motif analysis showing the top statistically significant motif analysis result (known or *de novo*) considering regions within −1 kb to +1 kb from the TSS.

profiling of mouse MCs produced by differentiating WT and $RelB^{-/-}$ bone marrow cells with GM-CSF + IL-4 or M-CSF, which generate primarily DCs or macrophages, respectively.[41,42] We then stimulated these cells with the TLR1/TLR2 or TLR9 agonists Pam3CSK4 (500 ng/mL) or CpG (0.1 μM) over a 24-hour time course and performed unbiased differential gene expression analyses followed by k-means clustering. Our analysis of GM-CSF MCs revealed 425 and 415 genes induced (log FC>1) with Pam3CSK4 and CpG, respectively. Differential gene expression analysis revealed clusters of genes that were hyperexpressed both in a basal state and after Pam3CSK4 or CPG stimulation (Fig 2, A and B). Pam3CSK4-stimulated genes in hyperexpressed cluster A (72 genes) showed average fold differences in expression ranging from 1.5× to 3.9× between $RelB^{-/-}$ and WT GM-CSF MCs at any of the measured time points (Fig 2, A and Table E2 in the Online Repository at www.jacionline.org). Likewise, CpG-stimulated genes in hyperexpressed cluster C (116 genes) showed average fold differences in expression ranging from 1.2× to 2.5× between $RelB^{-/-}$ and WT GM-CSF MCs at any of the measured time points (Fig 2, C and see Table E2), and they shared 55 of the 72 genes with Pam3CSK4 hyperexpressed cluster A. Motif enrichment analysis of hyperexpressed cluster A in Pam3CSK4-stimulated GM-CSF MCs revealed the ISRE as the top motif in a statistical enrichment analysis that considered regions within −1 kb to +1 kB from the TSS of the regulatory region of each gene (Fig 2, A [bottom]). Similarly, in CpG-stimulated GM-CSF MCs, hyperexpressed cluster C also yielded the ISRE as the top statistically enriched motif (Fig 2, C [bottom]). Furthermore, GO analysis of these clusters revealed ISG-inducing pathways, IFN-α response and IFN-γ response, as being among the top terms for both clusters. These data suggested that hyperexpressed genes in these clusters are ISGs, perhaps elevated by hyperinduction of interferons in $RelB^{-/-}$ GM-CSF MCs. We therefore analyzed a set of interferon genes and found *Ifnb1* to be elevated, with concurrent hyperexpression of the ISGs *Oasl*, *Oas1, Oas2, Ifit2,* and *Ifit3* in both Pam3CSK4- and CPG-stimulated conditions (Fig 2, C and D). Like poly(I:C)-stimulated RelB-null patient-derived fibroblasts, $RelB^{-/-}$ GM-CSF MCs stimulated with Pam3CSK4 also revealed a gene cluster (cluster B) that was hyperexpressed at the late hour 24–stimulated time point, with an average expression fold difference of 1.45× between $RelB^{-/-}$ and WT GM-CSF MCs. This cluster yielded NF-κB as the top result in motif enrichment analysis. All other clusters in both poly (I:C) and CpG were unchanged, containing average expression fold differences ranging from .9× to 1.17× between $RelB^{-/-}$ and WT GM-CSF MCs at all time points (Fig 2, A and C and see Table E2). Next, we asked whether myeloid cells differentiated with macrophage colony-stimulating factor (MCSF MCs) showed similar transcriptomic dysregulation as GM-CSF MCs. We generated MCSF MCs from $RelB^{-/-}$ and WT control bone marrow and undertook an analogous analysis following stimulation. We identified 1,243 unique LPS-induced genes (log FC > 1) and performed differential gene expression analysis. In contrast to our findings with GM-CSF MCs, our analysis of MCSF MCs revealed no differentially expressed gene clusters between WT and $RelB^{-/-}$ genotypes, with all clusters revealing average expression fold differences ranging from .9× to 1.1× between $RelB^{-/-}$ and WT MCSF MCs at all time points (Fig 2, E and see Table E2). The lack of expression phenotype may be because MCSF MCs show lower levels of *RelB* expression than GM-CSF MCs do.[38] Together, these results

indicated that the loss of RelB results in a cell-specific transcriptome phenotype, with PAMP-stimulated GM-CSF MCs showing broad and pronounced dysregulation of interferons and interferon-stimulated genes. Given the physiologic importance of DCs in both innate immunity as cytokine and chemokine producers[43] and adaptive immunity as antigen-presenting cells[44,45] as well as their demonstrated involvement in the $RelB^{-/-}$ autoinflammatory pathology,[23,24] we proceeded with $RelB^{-/-}$ GM-CSF MCs as a model system for further studies.

Compound deficiency of the type I interferon receptor ablates the hyperactivation of the interferon-stimulated gene program in RelB-deficient DCs

Although the expression of ISGs is driven primarily by the transcription factor complex ISGF3 or STAT1 homodimers (GAF), which are downstream of interferon signaling,[46] many ISGs also contain NF-κB motifs and have been shown to be regulated by NF-κB.[47-49] However, the potential role of NF-κB RelB in regulating ISGs or other immune response genes remains largely unknown. Given the hyperexpression of Ifnb1, whether hyperexpression of ISGs is caused by elevated IFN-β signaling and secondary ISGF3 activation or by interferon-independent regulatory mechanisms more directly caused by the loss of RelB remained unclear. To distinguish between these 2 mechanisms, we generated an $IFNAR^{-/-}RelB^{-/-}$ double-mutant mouse, which results in complete ablation of IFN-β signaling and thus a loss of secondary interferon-dependent gene expression programs, whereas interferon-independent gene expression remains. Using bone marrow from double-$IFNAR^{-/-}RelB^{-/-}$, single-$IFNAR^{-/-}$, single-$RelB^{-/-}$, and WT mice, we produced GM-CSF MCs and performed RNA-seq followed by differential gene expression analysis and k-means clustering.

To distinguish between interferon-dependent and interferon-independent dysregulated responses, we aimed to identify clusters with hyperexpressed genes shared between $RelB^{-/-}$ and $IFNAR^{-/-}RelB^{-/-}$ GM-CSF MCs and clusters that were not hyperexpressed in single-$IFNAR^{-/-}$ cells. We therefore first identified 1,123 induced (log FC > 1) genes upon CpG (0.1 μM) stimulation in WT or $RelB^{-/-}$ MCs and further filtered for genes that were hyperexpressed (FC > 1.5) in $RelB^{-/-}$ MCs versus in WT MCs. We identified 334 genes that met these criteria and then examined their expression patterns in $IFNAR^{-/-}$ and $IFNAR^{-/-}RelB^{-/-}$ MCs. Using k-means clustering on these genes of interest in our analysis, we identified hyperexpressed cluster A (215), which had average fold differences ranging from 1.8× to 2.1× between $IFNAR^{-/-}RelB^{-/-}$ MCs relative to WT MCs and 1.4× to 1.6× relative to single-$IFNAR^{-/-}$MCs at all observed time points (Fig 3, A and see Table E3 in the Online Repository at www.jacionline.org), suggesting that these may be genes directly affected by the loss of RelB and independent of interferon signaling. On the other hand, the induction of genes in hyperexpressed cluster B (119 genes) was lost in both $IFNAR^{-/-}RelB^{-/-}$ and single-$IFNAR^{-/-}$MCs, having average cpm FC differences of .6× in both $IFNAR^{-/-}RelB^{-/-}$ and $IFNAR^{-/-}$ MCs relative to WT MCs at the late hour 8–stimulated time point. These data suggested that genes in this cluster are ISGs and are hyperexpressed in $RelB^{-/-}$ owing to elevated IFN-β signaling. Motif enrichment analysis (within −1 kb to +1 kb from the TSS) of cluster A genes hyperexpressed specifically in $RelB^{-/-}$ and $IFNAR^{-/-}RelB^{-/-}$mutants revealed NF-κB as the top statistically
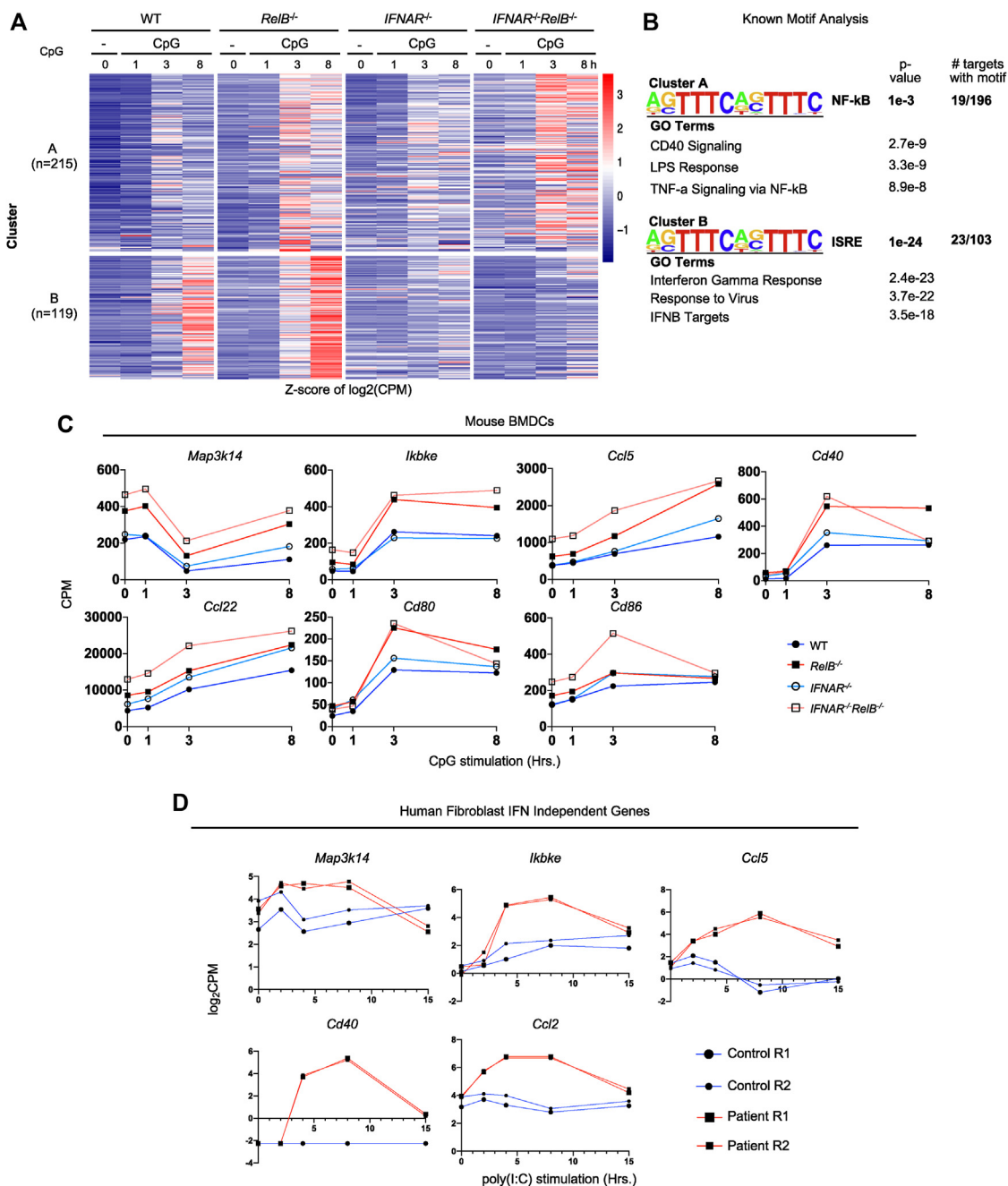
FIG 3. Type I interferon receptor compound deficiency ablates the elevated interferon-stimulated gene program but reveals other immune response genes suppressed by RelB independent of type I interferon signaling. **A,** Heatmap of *z*-scored cpm value of all *RelB*⁻/⁻ hyperexpressed genes in WT, *RelB*⁻/⁻, *IFNAR*⁻/⁻, and *IFNAR*⁻/⁻*RelB*⁻/⁻ MCs. Genes selected for CpG-induced (0.1 μM; log FC > 1) in WT or *RelB*⁻/⁻ MCs and hyperexpressed (FC > 1.5) in *RelB*⁻/⁻ MCs relative to WT MCs at any time point (334 genes). Each row represents individual genes, and each column is from an individual time point during stimulation. **B,** Top known motif analysis and GO results for gene clusters from (**A**). **C,** Line graphs of cpm values for interferon-independent hyperexpressed genes from cluster A from (**A**) and genes with similar functions during CpG stimulation (at 0, 1,3 , and 8 hours). Dark blue line (*closed circle*) represents WT GM-CSF MCs, dark red line (*closed square*) represents *RelB*⁻/⁻ GM-CSF MCs, light blue line (*open circle*) represents *IFNAR*⁻/⁻ GM-CSF MCs, and light red line (*open square*) represents *IFNAR*⁻/⁻*RelB*⁻/⁻ GM-CSF MCs. **D,** Line graphs of log₂ cpm values for genes from cluster A in Fig 3, *A* and genes with similar functions in patient-derived fibroblasts from Fig 1, *A*. Poly(I:C) stimulation (at 0, 2, 4, 8, and 15 hours). Blue line represents control patient–derived fibroblasts. Large circle represents replicate 1 (R1), small circle represents R2, red line represents fibroblasts derived from patient 1, large square represents R1, and small square represents R2. Motif analysis considered regions within –1 kb to +1 kb from the TSS. *BMDC*, Bone marrow–derived cell.
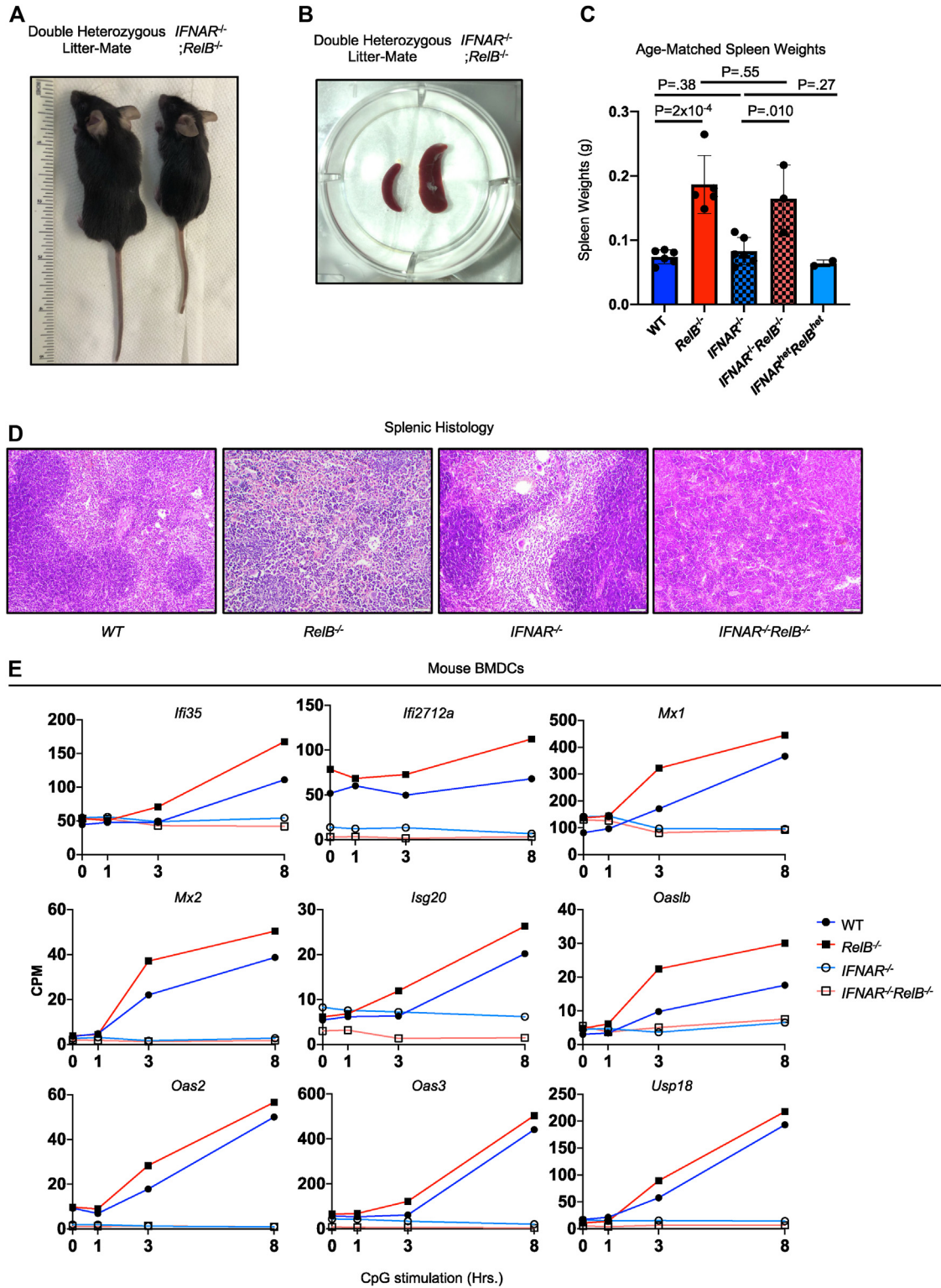
FIG 4. Ablation of the elevated type I interferon–stimulated gene program does not rescue RelB-null pathology. **A,** Representative image of IFNAR$^{-/-}$RelB$^{-/-}$ (*right*) and healthy litter mate (*left*) at 4 weeks of age. Ruler provided for scale. **B,** Representative image of spleens from IFNAR$^{-/-}$RelB$^{-/-}$ mice (*right*) and healthy litter mate (*left*). **C,** Spleen weights from age-matched WT (*solid dark blue*), RelB$^{-/-}$ (*solid dark red*), IFNAR$^{-/-}$ (*checkered light blue*), IFNAR$^{-/-}$RelB$^{-/-}$ (*checkered light red*), and IFNAR^{het}RelB^{het} (*solid light blue*) mice. Error bars indicate SD. Statistical analysis was done by using an unpaired 2-tailed Student *t* test. **D,** Representative images from histology of spleens from WT, RelB$^{-/-}$, IFNAR$^{-/-}$, and IFNAR$^{-/-}$RelB$^{-/-}$ mice demonstrating loss of white pulp and expansion of red pulp in IFNAR$^{-/-}$RelB$^{-/-}$ spleens. White bar is provided for scale (*bottom right*; 50 μm). **E,** Line graphs of gene expression (expressed as cpm values) for ISGs showing loss of

enriched motif, and GO analysis revealed the NF-κB-inducing pathways *CD40, TNF,* and *LPS-signaling* among the top terms (Fig 3, *B*). As expected, motif enrichment analysis of interferon-dependent cluster B revealed the ISRE as the top statistically enriched motif and GO analysis resulted in the ISG-inducing pathways *IFN-γ* and *IFN-β* as the top terms (Fig 3, *B*). Our analysis of MCs stimulated with poly(I:C) (10 μg/mL) also yielded an interferon-dependent cluster and interferon-independent cluster (see Fig E1 in the Online Repository at www.jacionline.org), with the interferon-dependent cluster sharing 44 of 82 genes with the CpG interferon-dependent cluster and the interferon-independent clusters sharing 58 of 130 genes (see Tables E3 and E4 in the Online Repository at www.jacionline.org).

These data suggested that although there are ISGs that are indirectly hyperexpressed by the loss of RelB, genes directly dysregulated by the loss of RelB are primarily NF-κB–regulated immune response genes. Analysis of individual genes within the interferon-independent cluster A and genes with similar interferon-independent expression patterns revealed a myriad of NF-κB–regulated proinflammatory genes, including the inflammatory chemokines *Ccl5* and *Ccl22,* the costimulatory molecules *Cd80 and Cd86,* and the canonic and noncanonic NF-κB–stimulating receptor *Cd40,* as well as the interferon signaling activators and p-IRF3 kinases *Map3k14* (NIK), and *Ikbke* (IKKε)[50,51] (Fig 3, *C*). We found that these genes were also hyperexpressed in *IFNAR*^{−/−}*RelB*^{−/−} MCs after poly (I:C) stimulation (see Fig E2 in the Online Repository at www.jacionline.org). We then asked whether these genes might also be hyperexpressed in RelB-null patient samples; we found 51 of 334 of these genes were hyperexpressed in human RelB-null fibroblasts from patient 1 (Fig 3, *D*). Together, these data suggest that although the ISG transcriptome signature is a substantial portion of the hyperexpression in RelB-null immune sentinel cells, RelB loss also results in hyperexpression of many immune response genes via interferon-independent mechanisms.

Ablation of the elevated type I interferon–stimulated gene program does not rescue RelB-null pathology

Having established that a significant proportion of the hyperexpressed genes associated with RelB loss are due to elevated interferon signaling, we asked whether these genes cause or contribute to the inflammatory pathology described for the *RelB*^{−/−} mouse. To answer this question, we examined the health state of *RelB*^{−/−} and *IFNAR*^{−/−}*RelB*^{−/−} double-mutant mice, as well as that of controls. After phenotypic analysis, the 4-week-old *IFNAR*^{−/−}*RelB*^{−/−} mouse appeared runted, much smaller than its healthy heterozygous littermate, and similar to *RelB*^{−/−} mice[22] (Fig 4, *A*). *IFNAR*^{−/−}*RelB*^{−/−} mice were found to have marked splenomegaly similar to that of *RelB*^{−/−} mice[22] (Fig 4, *B*). The spleens from *IFNAR*^{−/−}*RelB*^{−/−} mice weighed 2.9× and 2.5× more than the spleens from WT and single-*IFNAR*^{−/−} mice, respectively (Fig 4, *C*). Additionally, histologic analysis of spleens from *IFNAR*^{−/−}*RelB*^{−/−} mice revealed marked red pulp expansion and a

reduction in white pulp, similar to both our observations and prior reported findings in the *RelB*^{−/−} mice[22] (Fig 4, *D*). Assessment of the serum cytokine levels of *RelB*^{−/−} mice revealed elevated levels of CXCL10 and IL-6 (P = .051), consistent with previous reports regarding cytokine levels in the skin and lungs of *RelB*^{−/−} mice, respectively.[23,52] However, the levels of these elevated cytokines in the serum were not diminished by *IFNAR* deletion (see Fig E3). Together, these data identify 2 unique classes of genes regulated by the NF-κB subunit RelB in immune sentinel cells relevant to human pathology: interferon-dependent ISGs and interferon-independent inflammatory genes. Most importantly, these data determine clinically relevant findings in understanding which genes play critical roles in loss of RelB autoinflammatory pathology. Although we have shown that the loss of RelB indirectly regulates ISGs via type I interferon signaling, these genes seem to play a superfluous role in critical aspects of the multiorgan inflammation seen in *RelB*^{−/−} mice; instead, RelB directly suppresses interferon-independent genes that are likely the critical drivers of inflammation by immune sentinel cells. These data inform future studies for clinical targets in treating loss of RelB and other autoimmune and autoinflammatory disorders.

DISCUSSION

Here we have reported a molecular characterization of autoinflammatory disease caused by RelB deficiency. Taking an unbiased approach via transcriptome analysis, we found that fibroblasts derived from patients with RelB deficiency showed hyperexpression of IFN-β and ISGs when exposed to the pattern recognition receptor agonist poly(I:C). This was also seen in mouse DCs (Fig 2, *A*) and found to be dependent on signaling via the type I interferon receptor IFNAR (Figs 1, *A* and 3, *A*). Initially, we expected to provide evidence to categorize the *RelB*^{−/−} null pathology as an interferonopathy-driven autoinflammatory disease, thereby providing a clinically relevant therapeutic target to ameliorate the autoinflammatory pathology. However, we found that compound knockout *IFNAR*^{−/−}*RelB*^{−/−} mice showed no amelioration of critical aspects of the autoinflammatory disease characteristic of RelB-deficient mice. Like *RelB*^{−/−} mice, compound knockouts remained drastically runted, presented hunched backs, and had enlarged abdomens.[22] Additionally, no improvement in their organ inflammation, as measured by splenomegaly or histologic analysis of red and white pulp, was seen.

Given the pronounced ISG expression signature in RelB-deficient human fibroblasts and murine DCs, this is a surprising result. We wondered whether the compound mutant might have residual ISG expression via STAT1- or IRF3-dependent compensatory mechanisms[53,54]; however, detailed analysis confirmed that ISG expression was diminished to baseline or below by the *IFNAR* knockout mutation (Fig 4, *E*). Thus, despite being associated with a pronounced interferon signature, the pathology in C57/Bl6 mice resulting from RelB deficiency is not an interferonopathy. However, given that our studies were done with a specific congenic mouse strain under pathogen-free conditions, we cannot rule out type I interferon involvement in RelB knockout

induction in *IFNAR*^{−/−} (*light blue open circle*) and *IFNAR*^{−/−}*RelB*^{−/−} (*light red open square*) mice during CpG stimulation (at 0, 1, 3, and 8 hours). Dark blue line (*closed circle*) represents WT GM-CSF MCs, dark red line (*closed square*) represents *RelB*^{−/−} GM-CSF MCs, light blue line (*open circle*) represents *IFNAR*^{−/−} GM-CSF MCs, light red line (*open square*) represents *IFNAR*^{−/−}*RelB*^{−/−} GM-CSF MCs.

pathologies in other genetic backgrounds or in the context of diverse microbial exposure, which may be relevant to human pathology.[55] Additionally, we cannot rule out the potential role of other classes of interferons, given that our approach was restricted to deletion of type I interferon signaling.

What may be causing or contributing to the pathology if elevated ISGs are not? We focused our attention to interferon-independent genes with levels that remain elevated when *IFNAR* was also knocked out. We identified a group of proinflammatory genes with levels that were elevated in RelB-null patient-derived fibroblasts, as well as in murine *RelB*^{−/−} DCs. Importantly, this gene cluster remained elevated in DCs derived from *IFNAR*^{−/−}*RelB*^{−/−} mice. Our analysis of this cluster of dysregulated genes revealed the NF-κB motif as the top motif enriched near the regulatory regions of these genes. Interestingly, in fibroblasts from patients in a different family in which *RelB* expression is reduced but not absent, a cluster of hyperinduced genes also showed enrichment of the NF-κB motif,[19] which supports the notion that RelB deficiency leads to a pathology that can be categorized as a relopathy.

These dysregulated genes associated with the RelB relopathy include the potent proinflammatory chemokines *Ccl5* and *Ccl22*. Ccl5 is a potent regulator of inflammation and chemotaxis, and it is of great therapeutic interest in diseases involving immune dysregulation such as inflammatory bowel disease, atherosclerosis, hepatic inflammation, and many cancers.[56] Importantly, Ccl5 is a potent recruiter of T cells into sites of inflammation, and it can also recruit macrophages, eosinophils, and basophils.[57] Given that MCs reside in all peripheral tissues[58] and fibroblasts are found in most tissues of the body,[59] *Ccl5*-hyperexpressing fibroblasts and GM-CSF MCs in *RelB*^{−/−} mice and human patients may explain the initial recruitment of lymphocytes into inflamed organ tissues. MCs are also professional antigen-presenting cells responsible for initiating antigen-specific T-cell immunity. T cells require a secondary costimulation signal after T-cell receptor binding to become active, of which CD80, CD86, and CD40 are key costimulatory signaling molecules.[60,61] The hyperexpression of *CD80*, *CD86*, and *CD40* in *IFNAR*^{−/−}*RelB*^{−/−} GM-CSF MCs, suggests that these cells may exist in an intrinsic autoinflammatory state that may hyperactivate T-cell–mediated immune response at sites of inflammation in *RelB*^{−/−} mice. This is consistent with findings in RelB-null human patients of high peripheral T-cell numbers with clonally expanded populations, as shown by T-cell receptor–Vb analysis,[20,21] along with previous reports demonstrating that the multiorgan inflammation, myeloid hyperplasia, and inflammatory skin lesions are T-cell–dependent mechanisms in *RelB*^{−/−} mice.[52,62] In addition, the cluster of interferon-independent *RelB*^{−/−} dysregulated genes included *Ikbke* and the noncanonic NF-κB activator *Map3k14*, both of which are established type I interferon inducers,[51,63] prompting the question of whether they might contribute to the onset of interferon dysregulation. However, because our data indicated that the type I interferon ISG expression program is not contributing to the autoinflammatory pathology, this question was not pursued further.

In clinical settings, hyperexpression of ISGs, a hallmark of interferonopathies, has been associated with hepatosplenomegaly, meningoencephalitis, interstitial lung disease, recurrent unexplained fever, inflammatory organ damage, high mortality, and autoimmune characteristics,[18,64,65] some of which are symptoms seen in the *RelB*^{−/−} pathology. Clinical diagnosis of interferonopathies relies on an "interferon score" obtained by measuring the expression of a panel of interferon-stimulated genes,[66] a type I interferon response gene score, cytokine profiling, clinical phenotyping, or next-generation sequencing.[8] Testing of therapeutic targets along the interferon axis in many human trials showed moderate success with mAbs against IFNAR in treating systemic lupus erythematosus (SLE),[67] a well-characterized interferonopathy.[68] However, patient response rates remained less than 50%, and many other clinical anti-interferon trials have produced mixed results.[64] In the mouse, lupus models have a higher level of success with anti-IFNAR antibody therapy, extending survival from approximately 20% in controls to approximately 70% with treatment[69] and thus raising the question of what may account for the large variation in response to anti-interferon therapy.

Interestingly, in multiple studies, patients with SLE have also been characterized as having A20 haploinsufficiency, an auto-inflammatory relopathy presenting with systemic inflammation and increased NF-κB–mediated proinflammatory cytokines[70,71]; however, these studies did not test for an interferon signature. A separate study characterizing 30 patients with mutations in the *TNFAIP3* gene (encoding A20) and 8 other clinically diagnosed patients with A20 haploinsufficiency showed that many of these patients were previously diagnosed with diseases associated with interferonopathies and other inflammatory mechanisms such as SLE, autoimmune hepatitis, and juvenile idiopathic arthritis.[72-74]

Our studies presented here and by Sharfe et al[19] indicate that in RelB-deficient autoimmunity a presentation of interferonopathy is secondary to relopathy-type autoinflammatory mechanisms, establishing a hierarchic relationship. Although prior molecular characterization of human monogenic or polygenic pathologies suggests similarities to RelB deficiency in the presentation of the pathology, whether the described molecular mechanisms and hierarchy apply remains unclear. Yet, these findings may provide a potential explanation for the lack of response by patients with interferonopathy to therapeutics that target the interferon axis.[75] In sum, our findings emphasize the fact that a presentation of interferonopathy does not necessarily render the interferon pathway an effective drug target, and they underscore the need for continued characterization of NF-κB–driven autoinflammatory mechanisms to develop effective therapies for relopathies.

Data availability statement

The experimental data are available on the Gene Expression Omnibus website (accession no. GSE224515 and GSE34990) as well as in the Supplementary Data (in the Online Repository at www.jacionline.org).

DISCLOSURE STATEMENT

Disclosure of potential conflict of interest: The authors declare that they have no relevant conflicts of interest.

Key messages

- **Human and mouse NF-κB RelB deficiency leads to multi-organ autoimmune pathology.**
- **Unbiased profiling of patient-derived fibroblasts reveals a broad interferon gene signature that is also present in RelB knockout mouse DCs.**
- **Compound deficiency of the interferon type I receptor completely ablates this gene program but does not diminish RelB knockout autoimmune pathology, ruling out interferonopathy.**

REFERENCES

1. Committee for the Assessment of NIH Research on Autoimmune Diseases, Board on Population Health and Public Health Practice, Health and Medicine Division, National Academies of Sciences, Engineering, and Medicine. Enhancing NIH research on autoimmune disease. Washington, DC: National Academies Press; 2022. Available at: http://www.ncbi.nlm.nih.gov/books/NBK580299/. Accessed November 2, 2022.
2. Savic S, Coe J, Laws P. Autoinflammation: interferonopathies and other autoinflammatory diseases. J Invest Dermatol 2022;142:781-92.
3. Ancient missense mutations in a new member of the RoRet gene family are likely to cause familial Mediterranean fever. The International FMF Consortium. Available at: https://pubmed.ncbi.nlm.nih.gov/9288758/. Accessed November 2, 2022.
4. Shoham NG, Centola M, Mansfield E, Hull KM, Wood G, Wise CA, et al. Pyrin binds the PSTPIP1/CD2BP1 protein, defining familial Mediterranean fever and PAPA syndrome as disorders in the same pathway. Proc Natl Acad Sci U S A 2003;100:13501-6.
5. Romberg N, Al Moussawi K, Nelson-Williams C, Stiegler AL, Loring E, Choi M, et al. Mutation of NLRC4 causes a syndrome of enterocolitis and autoinflammation. Nat Genet 2014;46:1135-9.
6. Lam MT, Coppola S, Krumbach OHF, Prencipe G, Insalaco A, Cifaldi C, et al. A novel disorder involving dyshematopoiesis, inflammation, and HLH due to aberrant CDC42 function. J Exp Med 2019;216:2778-99.
7. Gavazzi F, Cross ZM, Woidill S, McMann JM, Rand EB, Takanohashi A, et al. Hepatic involvement in Aicardi-Goutières syndrome. Neuropediatrics 2021;52:441-7.
8. Arakelyan A, Nersisyan L, Poghosyan D, Khondkaryan L, Hakobyan A, Löffler-Wirth H, et al. Autoimmunity and autoinflammation: a systems view on signaling pathway dysregulation profiles. PLoS One 2017;12:e0187572.
9. Rood JE, Behrens EM. Inherited autoinflammatory syndromes. Annu Rev Pathol Mech Dis 2022;17:227-49.
10. Crow YJ, Black DN, Ali M, Bond J, Jackson AP, Lefson M, et al. Cree encephalitis is allelic with Aicardi-Goutiéres syndrome: implications for the pathogenesis of disorders of interferon alpha metabolism. J Med Genet 2003;40:183-7.
11. Crow YJ. Type I interferonopathies: a novel set of inborn errors of immunity. Ann N Y Acad Sci 2011;1238:91-8.
12. Isaacs A, Lindenmann J. Virus interference. I. The interferon. Proc R Soc Lond B Biol Sci 1957;147:258-67.
13. Ali S, Mann-Nüttel R, Schulze A, Richter L, Alferink J, Scheu S. Sources of type I interferons in infectious immunity: plasmacytoid dendritic cells not always in the driver's seat. Front Immunol 2019;10:778.
14. Knobeloch KP, Utermöhlen O, Kisser A, Prinz M, Horak I. Reexamination of the role of ubiquitin-like modifier ISG15 in the phenotype of UBP43-deficient mice. Mol Cell Biol 2005;25:11030-4.
15. Ritchie KJ, Malakhov MP, Hetherington CJ, Zhou L, Little MT, Malakhova OA, et al. Dysregulation of protein modification by ISG15 results in brain cell injury. Genes Dev 2002;16:2207-12.
16. Zhang X, Bogunovic D, Payelle-Brogard B, Francois-Newton V, Speer SD, Yuan C, et al. Human intracellular ISG15 prevents interferon-α/β over-amplification and auto-inflammation. Nature 2015;517:89-93.
17. Crow YJ, Zaki MS, Abdel-Hamid MS, Abdel-Salam G, Boespflug-Tanguy O, Cordeiro NJV, et al. Mutations in ADAR1, IFIH1, and RNASEH2B presenting as spastic paraplegia. Neuropediatrics 2014;45:386-91.
18. d'Angelo DM, Di Filippo P, Breda L, Chiarelli F. Type I Interferonopathies in children: an overview. Front Pediatr 2021;9:631329.
19. Sharfe N, Dalal I, Naghdi Z, Lefaudeux D, Vong L, Dadi H, et al. NFκB pathway dysregulation due to reduced RelB expression leads to severe autoimmune disorders and declining immunity. J Autoimmun 2022;102946.
20. Merico D, Sharfe N, Hu P, Herbrick JA, Roifman CM. RelB deficiency causes combined immunodeficiency. LymphoSign J 2015;2:147-55.
21. Sharfe N, Merico D, Karanxha A, Macdonald C, Dadi H, Ngan B, et al. The effects of RelB deficiency on lymphocyte development and function. J Autoimmun 2015;65:90-100.
22. Weih F, Carrasco D, Durham SK, Barton DS, Rizzo CA, Ryseck RP, et al. Multi-organ inflammation and hematopoietic abnormalities in mice with a targeted disruption of RelB, a member of the NF-κB/Rel family. Cell 1995;80:331-40.
23. Nair PM, Starkey MR, Haw TJ, Ruscher R, Liu G, Maradana MR, et al. RelB-deficient dendritic cells promote the development of spontaneous allergic airway inflammation. Am J Respir Cell Mol Biol 2018;58:352-65.
24. O'Sullivan BJ, Yekollu S, Ruscher R, Mehdi AM, Maradana MR, Chidgey AP, et al. Autoimmune-mediated thymic atrophy is accelerated but reversible in RelB-deficient mice. Front Immunol 2018;9:1092.
25. Liu Y, Wang X, Yang F, Zheng Y, Ye T, Yang L. Immunomodulatory role and therapeutic potential of non-coding RNAs mediated by dendritic cells in autoimmune and immune tolerance-related diseases. Front Immunol 2021;12:678918.
26. Smith T. Insights into the role of fibroblasts in human autoimmune diseases. Clin Exp Immunol 2005;141:388-97.
27. Ganguly D, Haak S, Sisirak V, Reizis B. The role of dendritic cells in autoimmunity. Nat Rev Immunol 2013;13:566-77.
28. Saha I, Jaiswal H, Mishra R, Nel HJ, Schreuder J, Kaushik M, et al. RelB suppresses type I interferon signaling in dendritic cells. Cell Immunol 2020;349:104043.
29. Ratra Y, Kumar N, Saha MK, Bharadwaj C, Chongtham C, Bais SS, et al. A vitamin D-RelB/NF-κB pathway limits Chandipura virus multiplication by rewiring the homeostatic state of autoregulatory type 1 IFN-IRF7 signaling [e-pub ahead of print]. J Immunol https://doi.org/10.4049/jimmunol.2101054. Accessed August 18, 2022.
30. Jin J, Hu H, Li HS, Yu J, Xiao Y, Brittain GC, et al. Noncanonical NF-κB pathway controls the production of type I interferons in antiviral innate immunity. Immunity 2014;40:342-54.
31. Cheng CS, Behar MS, Suryawanshi GW, Feldman KE, Spreafico R, Hoffmann A. Iterative modeling reveals evidence of sequential transcriptional control mechanisms. Cell Syst 2017;4:330-43.e5.
32. Martin M. Cutadapt removes adapter sequences from high-throughput sequencing reads. EMBnet.journal 2011;17:10-2.
33. Dobin A, Davis CA, Schlesinger F, Drenkow J, Zaleski C, Jha S, et al. STAR: ultrafast universal RNA-seq aligner. Bioinforma Oxf Engl 2013;29:15-21.
34. Twelve years of SAMtools and BCFtools. (Giga)ⁿScience Press. Available at: https://academic.oup.com/gigascience/article/10/2/giab008/6137722. Accessed September 29, 2022.
35. Liao Y, Smyth GK, Shi W. featureCounts: an efficient general purpose program for assigning sequence reads to genomic features. Bioinformatics 2014;30:923-30.
36. Frankish A, Diekhans M, Ferreira AM, Johnson R, Jungreis I, Loveland J, et al. GENCODE reference annotation for the human and mouse genomes. Nucleic Acids Res 2019;47:D766-73.
37. Robinson MD, McCarthy DJ, Smyth GK. edgeR: a Bioconductor package for differential expression analysis of digital gene expression data. Bioinformatics 2010;26:139-40.
38. Shih VFS, Davis-Turak J, Macal M, Huang JQ, Ponomarenko J, Kearns JD, et al. Control of RelB during dendritic cell activation integrates canonical and noncanonical NF-κB pathways. Nat Immunol 2012;13:1162-70.
39. Sen S, Cheng Z, Sheu KM, Chen YH, Hoffmann A. Gene regulatory strategies that decode the duration of NFκB dynamics contribute to LPS- versus TNF-specific gene expression. Cell Syst 2020;10:169-82.e5.
40. Schneider WM, Chevillotte MD, Rice CM. Interferon-stimulated genes: a complex web of host defenses. Annu Rev Immunol 2014;32:513-45.
41. Lutz MB, Kukutsch N, Ogilvie AL, Rössner S, Koch F, Romani N, et al. An advanced culture method for generating large quantities of highly pure dendritic cells from mouse bone marrow. J Immunol Methods 1999;223:77-92.
42. Assouvie A, Daley-Bauer LP, Rousselet G. Growing murine bone marrow-derived macrophages. In: Rousselet G, editorMacrophages: methods and protocols. New York, NY: Springer; 2018. pp. 29-33.
43. Blanco P, Palucka AK, Pascual V, Banchereau J. Dendritic cells and cytokines in human inflammatory and autoimmune diseases. Cytokine Growth Factor Rev 2008;19:41-52.
44. Hilligan KL, Ronchese F. Antigen presentation by dendritic cells and their instruction of CD4+ T helper cell responses. Cell Mol Immunol 2020;17:587-99.
45. Embgenbroich M, Burgdorf S. Current concepts of antigen cross-presentation. Front Immunol 2018;9:1643.
46. Wang W, Xu L, Su J, Peppelenbosch MP, Pan Q. Transcriptional regulation of antiviral interferon-stimulated genes. Trends Microbiol 2017;25:573-84.
47. Cheng CS, Feldman KE, Lee J, Verma S, Huang DB, Huynh K, et al. The specificity of innate immune responses is enforced by repression of interferon response elements by NF-κB p50. Sci Signal 2011;4:ra11.
48. Pfeffer LM, Kim JG, Pfeffer SR, Carrigan DJ, Baker DP, Wei L, et al. Role of nuclear factor-κB in the antiviral action of interferon and interferon-regulated gene expression. J Biol Chem 2004;279:31304-11.

49. Wei L, Sandbulte MR, Thomas PG, Webby RJ, Homayouni R, Pfeffer LM. NFκB negatively regulates interferon-induced gene expression and anti-influenza activity. J Biol Chem 2006;281:11678-84.

50. Fitzgerald KA, McWhirter SM, Faia KL, Rowe DC, Latz E, Golenbock DT, et al. IKKε and TBK1 are essential components of the IRF3 signaling pathway. Nat Immunol 2003;4:491-6.

51. Parvatiyar K, Pindado J, Dev A, Aliyari SR, Zaver SA, Gerami H, et al. A TRAF3-NIK module differentially regulates DNA vs RNA pathways in innate immune signaling. Nat Commun 2018;9:2770.

52. Barton D, HogenEsch H, Weih F. Mice lacking the transcription factor RelB develop T cell-dependent skin lesions similar to human atopic dermatitis. Eur J Immunol 2000;30:2323-32.

53. Ashley CL, Abendroth A, McSharry BP, Slobedman B. Interferon-independent innate responses to cytomegalovirus. Front Immunol 2019;10:2751.

54. Ashley CL, Abendroth A, McSharry BP, Slobedman B. Interferon-independent up-regulation of interferon-stimulated genes during human cytomegalovirus infection is dependent on IRF3 Expression. Viruses 2019;11:246.

55. Rutherford HA, Kasher PR, Hamilton N. Dirty fish versus squeaky clean mice: dissecting interspecies differences between animal models of interferonopathy. Front Immunol 2021;11:623650.

56. Zeng Z, Lan T, Wei Y, Wei X. CCL5/CCR5 axis in human diseases and related treatments. Genes Dis 2022;9:12-27.

57. Lv D, Zhang Y, Kim HJ, Zhang L, Ma X. CCL5 as a potential immunotherapeutic target in triple-negative breast cancer. Cell Mol Immunol 2013;10:303-10.

58. Castell-Rodríguez A, Piñón-Zárate G, Herrera-Enríquez M, Jarquín-Yáñez K, Medina-Solares I, Castell-Rodríguez A, et al. Dendritic cells: location, function, and clinical implications. In: Ghosh A, editor. Biology of myelomonocytic cells. London, UK: IntechOpen; 2017. Accessed November 5, 2022.

59. McAnulty RJ. Fibroblasts and myofibroblasts: their source, function and role in disease. Int J Biochem Cell Biol 2007;39:666-71.

60. Carenza C, Calcaterra F, Oriolo F, Di Vito C, Ubezio M, Della Porta MG, et al. Costimulatory molecules and immune checkpoints are differentially expressed on different subsets of dendritic cells. Front Immunol 2019 [cited 2022 Nov 5];10:1325.

61. Hubo M, Trinschek B, Kryczanowsky F, Tüttenberg A, Steinbrink K, Jonuleit H. Costimulatory molecules on immunogenic versus tolerogenic human dendritic cells. Front Immunol 2013;4:82.

62. Weih F, Durham SK, Barton DS, Sha WC, Baltimore D, Bravo R. Both multiorgan inflammation and myeloid hyperplasia in RelB-deficient mice are T cell dependent. J Immunol 1996;157:3974-9.

63. Hemmi H, Takeuchi O, Sato S, Yamamoto M, Kaisho T, Sanjo H, et al. The roles of two IκB kinase-related kinases in lipopolysaccharide and double stranded RNA signaling and viral infection. J Exp Med 2004;199:1641-50.

64. Sanchez GAM, Reinhardt A, Ramsey S, Wittkowski H, Hashkes PJ, Berkun Y, et al. JAK1/2 inhibition with baricitinib in the treatment of autoinflammatory interferonopathies. J Clin Invest 2018;128:3041-52.

65. Jaan A, Rajnik M. TORCH complex. In: StatPearls. Treasure Island. FL: StatPearls Publishing; 2022.

66. Rice GI, Melki I, Frémond ML, Briggs TA, Rodero MP, Kitabayashi N, et al. Assessment of type I interferon signaling in pediatric inflammatory disease. J Clin Immunol 2017;37:123-32.

67. Morand EF, Furie R, Tanaka Y, Bruce IN, Askanase AD, Richez C, et al. Trial of anifrolumab in active systemic lupus erythematosus. N Engl J Med 2020;382:211-21.

68. Volpi S, Picco P, Caorsi R, Candotti F, Gattorno M. Type I interferonopathies in pediatric rheumatology. Pediatr Rheumatol 2016;14:35.

69. Baccala R, Gonzalez-Quintial R, Schreiber RD, Lawson BR, Kono DH, Theofilopoulos AN. Anti-IFNAR antibody treatment ameliorates disease in lupus-predisposed mice. J Immunol 2012;189:5976-84.

70. Zhou Q, Wang H, Schwartz DM, Stoffels M, Park YH, Zhang Y, et al. Loss-of-function mutations in TNFAIP3 leading to A20 haploinsufficiency cause an early-onset autoinflammatory disease. Nat Genet 2016;48:67-73.

71. Aeschlimann FA, Batu ED, Canna SW, Go E, Gül A, Hoffmann P, et al. A20 haploinsufficiency (HA20): clinical phenotypes and disease course of patients with a newly recognised NF-kB-mediated autoinflammatory disease. Ann Rheum Dis 2018;77:728-35.

72. Clarke SLN, Robertson L, Rice GI, Seabra L, Hilliard TN, Crow YJ, et al. Type 1 interferonopathy presenting as juvenile idiopathic arthritis with interstitial lung disease: report of a new phenotype. Pediatr Rheumatol 2020;18:37.

73. Kadowaki T, Ohnishi H, Kawamoto N, Hori T, Nishimura K, Kobayashi C, et al. Haploinsufficiency of A20 causes autoinflammatory and autoimmune disorders. J Allergy Clin Immunol 2018;141:1485-8.e11.

74. Gedik KC, Lamot L, Romano M, Demirkaya E, Piskin D, Torreggiani S, et al. The 2021 European Alliance of Associations for Rheumatology/American College of Rheumatology points to consider for diagnosis and management of autoinflammatory type I interferonopathies: CANDLE/PRAAS, SAVI and AGS. Ann Rheum Dis 2022;81:601-13.

75. Paredes JL, Niewold TB. Type I interferon antagonists in clinical development for lupus. Expert Opin Investig Drugs 2020;29:1025-41.